

# 1 Is waveform worth it? A comparison of LiDAR approaches 2 for vegetation and landscape characterisation.

3  
4 Karen Anderson<sup>1\*</sup>, Steven Hancock<sup>1</sup>, Mathias Disney<sup>2</sup> and Kevin J. Gaston<sup>1</sup>

5 \* Corresponding author: [Karen.Anderson@exeter.ac.uk](mailto:Karen.Anderson@exeter.ac.uk)

6 <sup>1</sup> Environment and Sustainability Institute, University of Exeter, Penryn Campus, TR10 9FE,  
7 UK

8 <sup>2</sup> University College London, Department of Geography, Gower Street, London, WC1E 6BT  
9 and National Centre for Earth Observation (NCEO)

10 **Keywords:** LiDAR, vegetation, waveform, structure, validation, urban

11 **Running title:** Waveform LiDAR considerations in ecology

---

## 12 **Abstract**

13 Light Detection And Ranging (LiDAR) systems are frequently used in ecological studies to  
14 measure vegetation canopy structure. Waveform LiDAR systems offer new capabilities for  
15 vegetation modelling by measuring the time-varying signal of the laser pulse as it illuminates  
16 different elements of the canopy, providing an opportunity to describe the 3D structure of  
17 vegetation canopies more fully. This paper provides a comparison between waveform  
18 airborne laser scanning (ALS) data and discrete return ALS data using terrestrial laser  
19 scanning (TLS) data as an independent validation. With reference to two urban landscape  
20 typologies we demonstrate that discrete return ALS data provided more biased and less  
21 consistent measurements of woodland canopy height (in a 100% tree covered plot, height  
22 underestimation bias = 0.82 m; SD = 1.78m) than waveform ALS data (height overestimation  
23 bias = -0.65 m; SD = 1.45 m). The same biases were found in suburban data (in a plot  
24 consisting of 100% hard targets e.g. roads and pavements), but discrete return ALS were  
25 more consistent here than waveform data (SD = 0.57 m compared to waveform SD = 0.76  
26 m). Discrete return ALS data performed poorly in describing the canopy understorey  
27 compared to waveform data. Results also highlighted errors in discrete return ALS intensity,  
28 which were not present with waveform data. Waveform ALS data therefore offer an improved  
29 method for measuring the three dimensional structure of vegetation systems but carry a  
30 higher data processing cost. New toolkits for analysing waveform data will expedite future  
31 analysis and allow ecologists to exploit the information content of waveform LiDAR.

32

## 33 1. Introduction

34 The spatial and volumetric structure of vegetation in ecosystems is a key driver of function  
35 (Shugart et al., 2010) and Light Detection And Ranging (LiDAR) instruments provide critical  
36 data for describing and modelling vegetation structure (Vierling et al., 2008). LiDAR  
37 instruments can be operated from the ground (e.g. Terrestrial Laser Scanning; TLS) from  
38 airborne platforms (e.g. Airborne Laser Scanning; ALS) or from satellites (e.g. freely  
39 available data from ICESat (Harding and Carabajal, 2005)), and come in two forms –  
40 discrete return and full waveform systems (Lefsky et al., 2002, Vierling et al., 2008). The  
41 difference between these is the way in which data are recorded. Discrete return systems  
42 (most commonly used) measure the time taken for a laser pulse to travel to an object and  
43 are used to determine height. In products derived from ALS data there are usually two  
44 datasets: a digital surface model (DSM) provides an estimate of the top-of-canopy height  
45 whilst the digital terrain model (DTM) shows topographic variability in the neighbouring  
46 ground surface. Such data can be used to describe canopy patterns (Anderson et al., 2010,  
47 Luscombe et al., 2014), model hydrological flowpaths (Jones et al., 2014), monitor wildlife  
48 habitat (Hyde et al., 2006), or produce carbon inventories at patch (Calders et al., 2015) or  
49 landscape (Asner et al., 2011) scales. Waveform ALS data (Figure 1), however, have the  
50 potential to provide much richer spatial information about canopy characteristics in three  
51 dimensions. This is because these systems record the range to multiple targets within the  
52 canopy (Danson et al., 2014). By measuring the time-varying signal of the laser pulse as it  
53 illuminates different elements of the canopy, these systems can be used to model the spatial  
54 character and arrangement of structures that drive canopy biophysical processes such as  
55 canopy architecture and size and woody biomass (Armston et al., 2013, Mallet and Bretar,  
56 2009) and can provide useful data for studies requiring tree species discrimination (Alonzo et  
57 al., 2014).

58 It is only since around 2010 that waveform systems have begun to be heavily explored in  
59 ecological contexts (with limited earlier examples by Anderson et al. (2006), and Hyde et al.  
60 (2005), for example). This is probably because of the high data volumes requiring high  
61 computing power, and the complexity of analysing the return signal (e.g. rather than a few  
62 'hits' (typically, up to five) from a discrete return system, waveform systems give a near-  
63 continuous pulse; Figure 1). Waveform data represent a significant signal processing task -  
64 tracing the photon from the sensor to the ground and understanding what the interactions  
65 represent is a potential barrier to their application in ecology and beyond. Extracting 3D  
66 canopy information from the waveform is challenging because the pulse can be perturbed on  
67 its path through the canopy – e.g. the electromagnetic radiation in the pulse can be  
68 redirected within the canopy and is known to suffer 'multiple scattering' between different

69 elements (e.g. leaves and woody biomass). This leads to highly complex signals requiring  
70 de-noising and correction using signal processing approaches, followed by product  
71 validation. Despite this challenge there are a variety of new waveform signal processing  
72 approaches emerging, particularly for vegetation applications, with most studies following  
73 one of three methods:

74 1) Decomposition into points and attributes using function fitting (Hofton et al., 2000,  
75 Wagner et al., 2008);

76 2) Decomposition into points using deconvolution (Jiaying et al., 2011, Roncat et al.,  
77 2011, Hancock et al., 2008);

78 3) Extracting metrics such as height of median energy (Drake et al., 2002).

79 The points or metrics from the resulting models can then be used to infer plot-level  
80 characteristics or calculate canopy height (Boudreau et al., 2008), fit geometric primitives to  
81 crowns (Lindberg et al., 2012); or fill voxels to enable construction of 3-dimensional models  
82 from a regular grid of cubes (e.g. as in Minecraft) where canopy structure can be optimally  
83 modelled (Hosoi et al., 2013).

84 Waveform laser scanning technology is now at a tipping point, evidenced by NASA's  
85 forthcoming 'Global Ecosystem Dynamics Investigation LiDAR' space mission, due for  
86 launch in 2018 (GEDI (NASA, 2014, Krainak et al., 2012)). It is hoped that the enhanced  
87 capability of the waveform system on GEDI will provide superior global estimates of  
88 vegetation carbon stocks.

89 In this paper we address the pragmatic research question of what benefits waveform ALS  
90 data can offer ecologists over more easily obtainable discrete return ALS products, using  
91 urban systems as an exemplar. Quantitative description of the pattern and 3D structure of  
92 urban vegetation demands fine-scale spatially-distributed information describing canopy  
93 architecture (Yan et al., 2015). This is because the pattern and extent of green infrastructure  
94 (e.g. street trees, parks, domestic yards and gardens) is a key determinant of the provision  
95 of ecosystem services in cities and towns, including nutrient cycling, temperature and flood  
96 risk regulation, reduction in atmospheric pollution, aesthetics, and multiple dimensions of  
97 human health (Gaston et al., 2013). Most examples of remote sensing approaches for  
98 mapping urban greenspace rely on either optical classification of aerial photographs, or  
99 height-based classification of discrete return ALS to determine the spatial distribution of  
100 basic classes such as trees, bushes and grass (Yan et al., 2015, Chen et al., 2014). Whilst  
101 these data are appropriate to the particular scale range of the texture of urban vegetation  
102 variance, and allow the small patch sizes of urban greenspace to be mapped (e.g. in yards  
103 and gardens) they neglect to characterise the important vertical distribution of vegetation and

104 photosynthetic material through the depth of the canopy and its spatial form. Furthermore  
105 they cannot account for important habitat features such as the understorey which are  
106 important in driving urban ecological connectivity. This work sought to establish the impact of  
107 those omissions in describing urban vegetation complexity.

108 Here, we compare a simply processed waveform ALS product with discrete return ALS data  
109 from the perspective of ecologists working in urban environments. We validate the findings  
110 using a ground-based TLS survey, quantify differences in each approach and evaluate the  
111 relative processing costs of each. Finally, we discuss the wider implications for using  
112 waveform ALS data for vegetation monitoring in other ecological settings.

## 113 **2. Materials and Methods**

### 114 **2.1 ALS survey data**

115 An ALS survey was carried out over the town of Luton, UK on 5 and 6 September 2012  
116 (Figure 2) when the urban vegetation was in full leaf-on stage. The survey utilised the UK  
117 Natural Environment Research Council (NERC) Airborne Research and Survey Facility  
118 (ARSF) Dornier 228 aircraft platform and the Leica ALS50-II ALS system with a WDM65 full  
119 waveform digitiser, measuring at 1064 nm. Geo-registration of the scans was achieved using  
120 differential global positioning system (GPS) data from the aircraft and at a linked GPS  
121 ground-station. All ALS data were collected by a single instrument with separate discrete  
122 return and waveform output streams. The footprint density of ALS data (waveform and  
123 discrete return data) were collected with a density of between one point per 25 cm<sup>2</sup> and one  
124 point per 4 m<sup>2</sup> – this variability is normal and is dependent on scan angle and overlap  
125 between flight lines. The discrete return ALS data had up to four returns per pulse. Raw ALS  
126 data were processed into a geolocated point cloud with associated waveforms using Leica  
127 ALSPP software (version 2.75). More detailed documentation about the data processing can  
128 be found online (NERC ARSF, 2014a, NERC ARSF, 2014b)

129 Two data products from the ALS survey were compared: a discrete return ALS point cloud  
130 describing x,y,z spot heights and intensity; and a waveform ALS dataset which required pre-  
131 processing before it could be used.

### 132 **2.2 Field site description**

133 Data from two field validation sites (both within an area of Luton, UK, called Little  
134 Bramingham Woods) are presented in this manuscript (Figure 2). The first site was in an  
135 area of dense and varied tree cover with a clear understorey (referred to as the ‘woodland’  
136 site) and the second was from a residential area (referred to as the ‘suburban’ site). A very  
137 simple 2 m resolution land cover map (LCM) was generated for these sites using data from

138 an airborne hyperspectral survey (with the AISA Eagle 12 bit pushbroom scanner) carried  
139 out at the same time as the ALS survey. The LCM was generated by applying an  
140 unsupervised classification algorithm to discrete return ALS data and a Normalised  
141 Difference Vegetation Index (NDVI) product. The NDVI was calculated using equation 1  
142 where  $\rho_{vis}$  was the mean visible reflectance in channels from 500 nm to 680 nm and  $\rho_{nir}$  was  
143 the mean infrared reflectance between 761 nm and 961 nm.

$$NDVI = \frac{\rho_{nir} - \rho_{vis}}{\rho_{nir} + \rho_{vis}} \quad (1)$$

144

145 A 70 cm threshold for discriminating tall from short vegetation and an NDVI threshold of 0.2  
146 for discriminating vegetated from non-vegetated areas was used. In the woodland area, the  
147 LCM showed that the majority of the site was covered by tall vegetation. In the suburban  
148 area, as was expected, there was a mix of tall and short vegetation and vegetated and non-  
149 vegetated areas. For both woodland and suburban sites the discrete return and waveform  
150 ALS data were extracted for a 20 m by 20 m square at the centre of each TLS ground-  
151 validation site for comparison. These comparison areas were chosen because they were  
152 proximal to sampling sites where complementary ecological data were being collected –  
153 specifically bird feeders where population counts were being collected and where flows of  
154 biodiversity through urban systems were being measured. These sites were also evaluated  
155 in the waveform LiDAR datasets prior to collection of the TLS validation data, and were  
156 found to be representative areas with a variety of waveform shapes and widths.

### 157 **2.3 Method for processing waveform ALS data**

158 The ALS50-II system recorded the intensity of reflected light as an eight-bit value every 1  
159 nanosecond. The first step in signal processing the waveform data was to remove  
160 background electronic noise – which is known to be very stable in the Leica ALS50-II  
161 (Hancock et al., 2015). Here we used a simple method to extract canopy signals from the  
162 waveform ALS data. The first peak in the waveform above the noise threshold was traced  
163 back to the mean noise level (DN=12, derived from a histogram) to provide a consistent  
164 estimate of the canopy maxima. The histograms of signal intensity from Hancock et al.  
165 (2015) were then used to set the simple noise threshold at DN=16 (see Hancock et al.  
166 (2015) Figure 5b) to remove all background noise, and the result was a product showing  
167 point height information that could be used to compare datasets quantitatively. Further  
168 processing - for example using function fitting, deconvolution or pulse width subtraction may  
169 have further improved the retrieval of the 'true' canopy top (Hofton et al., 2000). These more  
170 complex signal processing methods were not the focus of this paper and will be discussed in

171 a subsequent manuscript which develops a validated voxel-based approach for 3-D canopy  
172 description in urban settings.

#### 173 **2.4 Validation data from TLS survey**

174 To validate the information content of the two ALS products, a waveform TLS system was  
175 deployed (Riegl VZ-400, operating at 1545 nm (near infra-red)) to measure vegetation  
176 structure (from the ground up) on 5 and 7 August 2014. The TLS instrument had a reported  
177 5 mm accuracy and 3 mm repeatability which was far greater than the ALS data. Previous  
178 work by Calders et al. (2015) has shown how this approach provides a good validation  
179 where accurate tree heights could be obtained, and demonstrating that attenuation was not  
180 significant. The dates of field sampling with TLS were chosen to ensure that the vegetation  
181 was in a similar state to the time of the ALS survey. Validation sites were chosen to cover a  
182 range of observed habitat structures, and a variety of ALS waveform shapes and urban  
183 typologies. As a result the TLS scan methodology had to be adapted for each site so as to  
184 capture the variability in canopy structure appropriately. The plot sizes also varied, with small  
185 (5 m) plots sometimes requiring three scan positions to capture variability in the dense  
186 vegetation whilst sparsely vegetated plots measuring tens of metres in size only required two  
187 scan positions due to reduced occlusion. Each site was scanned from two or three different  
188 positions so as to infill shadowed areas, and multiple scans were co-registered using  
189 reflector targets. TLS point clouds were then manually translated to align the roofs of  
190 buildings with the geolocated ALS data to within 10 cm vertically and < 30 cm horizontally.

#### 191 **2.5 Quantitative comparison**

192 To quantitatively compare the consistency of the height estimate error in the datasets, the  
193 mean difference between the ALS and TLS derived ranges to the tallest object, and the  
194 standard deviation (SD) of those differences were calculated for a 5 m x 5 m area around the  
195 plot centres of the 20 m x 20 m extracts. In the woodland area this 5 m x 5 m measurement  
196 area was covered with dense trees. The LCM classification indicated that the woodland plot  
197 comprised 100% tall vegetation. In the suburban zone, the 5 m x 5 m measurement area  
198 was a road surface with neighbouring pavement and lamp posts with no green elements.  
199 The LCM classification indicated that this plot comprised 75% short non-vegetation (e.g.  
200 roads, footpaths, gravel driveways or cars), and 25% tall non-vegetation (e.g. buildings or  
201 lamp posts). These comparison plots therefore represent endmembers of urban structural  
202 diversity and so offer the most effective insight into the relative merits of waveform versus  
203 discrete return ALS products.

204 The ALS waveform-derived canopy top was calculated using the method described in  
205 Hancock et al. (2011) using a mean noise level of 12 and a noise threshold of 16. Calders et  
206 al. (2015) have demonstrated that TLS-derived estimates of canopy height are very reliable  
207 (see figure 6 in (Calders et al., 2015)) and our comparisons therefore rely on TLS being able  
208 to provide a robust validation of true canopy height. Biases between TLS measuring the leaf-  
209 underside versus the ALS measuring the leaf-topside are treated as negligible here.

210

### 211 **3. Results**

#### 212 **3.1 Validation of airborne discrete return and waveform ALS data with TLS**

213 Figure 3 shows the results of comparing waveform and discrete return ALS data with TLS  
214 data. Over hard surfaces with little spatial complexity in height and structure, such as roads  
215 and buildings in the suburban area (Figure 3(a) and (b)), the discrete return data provided a  
216 height model that indicated basic trends, whilst the waveform data showed pulse blurring  
217 caused by the 3.55 nanosecond system pulse (Hancock et al., 2015). Conversely, the  
218 waveform pulses (coloured green) in Figure 3(b) travelled through urban greenspace  
219 components like bushes and shrubs and so provided potentially useful within-canopy  
220 structural information, whilst the discrete return points failed to capture the detail of the  
221 canopy profile.

222 In the woodland setting the ALS waveform system recorded returns from throughout the  
223 canopy and could be used to provide useful information on the canopy understorey (e.g.  
224 presence/absence, density and structure). In some settings there was penetration of the ALS  
225 waveform all the way to the ground, allowing the urban habitat to be described much more  
226 accurately than with discrete return data (Figure 3(c) and (d)). In some places, however,  
227 there were data shadows – e.g. beneath the centre of a large tree (Figure 3(d)). This same  
228 figure shows that in a few places the discrete return ALS heights of the tree tops appear to  
229 be under-estimated relative to the height derived from TLS. A few further issues are evident  
230 with the waveform data – in figure 3(b) and (d) some of the waveform returns appear below  
231 the TLS-derived ground surface. These errors are caused by the combination of multiple  
232 scattering of photons in the canopy and automatic instrument settings applied at the point of  
233 data collection. These erroneous points can be corrected using signal processing  
234 approaches (see section 1), but these are computationally complex and require extensive  
235 testing and validation.

236

237

238

239 **3.1.1 Quantitative comparison**

240 Applying the method explained in 2.3 and 2.4, statistics were generated that showed that  
241 discrete return ALS data consistently overestimated the range (and so underestimated  
242 height), with a bias of 0.82 m (SD = 1.78 m) in the 5 m x 5 m woodland test area. Conversely  
243 the waveform ALS data consistently underestimated range (and so overestimated height),  
244 but with a smaller bias, and provided a more consistent estimate of height (i.e. smaller SD)  
245 than the discrete return data (bias = -0.65 m; SD = 1.45 m). In the 5 m x 5 m suburban test  
246 area the biases showed similar patterns (discrete return bias = 0.78 m; waveform bias = -  
247 0.29 m) but the discrete return data had a lower SD (0.57 m) compared to the waveform  
248 data (0.76 m), indicating that more consistent results were achieved with discrete return data  
249 where vegetation was not present. This analysis adds weight to the suggestion that the  
250 discrete return algorithms are optimised for hard surfaces (such as roads), where they  
251 outperform simply processed waveform data, and that waveform data provide more accurate  
252 results over vegetation. It should be noted that the waveform ALS product could be  
253 processed to generate a product which performed as well as the discrete return data over  
254 hard surfaces, but the computational costs of doing so would be high.

255

256 **3.2 ALS intensity measures**

257 Further issues with discrete return ALS products are apparent when evaluating discrete  
258 return ALS intensity values over vegetated surfaces. Figure 4 demonstrates this by  
259 comparing the intensity measured from the discrete return ALS product with the reflected  
260 energy from the waveform data (the integral of the waveform intensity with time) over a  
261 mixed urban landscape in Luton. Areas of high intensity appear brighter than those with  
262 lower intensity. At 1064 nm healthy green vegetation would be expected to reflect radiation  
263 strongly and yet some of the vegetated areas in Figure 4(a) show low intensity (indicated by  
264 dark areas) which is an artefact of the diffuse return containing a large amount of energy but  
265 having a low, broad peak (Hancock et al., 2015). Therefore, there are often non-physical  
266 effects caused by signal distortion, and these could lead to large errors in interpretation of  
267 discrete return ALS data if used for automated land cover determination. This is frequently  
268 overlooked - for example studies by Antonarakis et al. (2008) and Donoghue et al. (2007)  
269 both utilised discrete return ALS intensity as an additional measure to derive a supervised  
270 classification of vegetation types. The discrete return intensity is a function of vegetation  
271 structure (e.g. foliage profile), albedo (e.g. phenology) and the processing algorithm applied,  
272 so will confound classification accuracy if one or more of those variables is changed.  
273 Waveform ALS data are much less prone to such limitations, being able to record a much  
274 more accurate measure of reflected radiation and shape of the signal response of the target,



275 allowing the same discrimination using the physically based shape rather than an artefact  
276 (Figure 4(b)).

277

### 278 **3.3 Computational requirements**

279 When deciding which ALS product to use one must consider data volumes and  
280 computational requirements underpinning information extraction. Data volume and  
281 processing costs are currently much higher with waveform data than with discrete return  
282 data. For example, the waveform files used here (LAS1.3 format (ASPRS, 2015)) were 6 to  
283 10 times larger than the discrete return (LAS1.0 format) files. For example, 1 strip of discrete  
284 return ALS data would occupy 700Mb of disk space, whilst the same spatial extent of  
285 waveform ALS data would occupy 4.2Gb. Much of this additional data volume is occupied by  
286 wavebins that contain no usable signal but which must be retained for post-processing.  
287 Once the background noise is removed, file sizes can be reduced by roughly an order of  
288 magnitude by simple run length encoding. The signal processing needed to extract target  
289 properties is computationally expensive: applying the method described in Hancock *et al.*  
290 (2008) took 25 processor days on a computer with a 3Ghz CPU, although this could be  
291 parallelised on a cluster workstation to expedite processing time. In comparison, the discrete  
292 return point cloud is processed by the instrument during collection and typically is ready for  
293 use in geographical information systems or other image processing software on delivery  
294 (although some users will subsequently choose to apply additional topographic normalisation  
295 techniques or post-process the data using other tools).

296

297 Whilst considering the various costs of extracting information from waveform ALS data, it is  
298 also important to highlight the recent development of new software tools for expeditious  
299 analysis of such data. Not all of these tools are mature but they offer a means by which most  
300 users could extract useful information from both discrete return and waveform-capable  
301 LiDAR systems (from both ALS and TLS systems). Such tools (we list only free-to-use (FTU)  
302 or open source (O/S) options) are briefly summarised in table 1.

### 303 **4. Summary and conclusions**

304 The results shown here suggest that discrete return ALS data are optimised for use in  
305 measurement of simple hard targets (i.e. roads), and that the methods and assumptions  
306 used to generate discrete return ALS products do not permit accurate description of the  
307 three dimensional structural complexity of vegetated areas. Using two urban landscape  
308 typologies we have shown that if discrete return data were used alone, measurements of the  
309 vegetation system would be biased in terms of canopy height (underestimation), inaccurate  
310 in terms of intensity (likely resulting in physical misclassifications of greenspace) and missing

311 vital data on the characteristics of the canopy understorey. Inaccuracies arising from the use  
312 of discrete return ALS data in measuring tree canopy height have been reported previously,  
313 for example by Zimble et al. (2003) who showed bias in deriving canopy height models from  
314 discrete return ALS (in this example, the underestimation was caused by the points missing  
315 tree tops, hitting the shoulders of tree crowns and thus, underestimating canopy height). The  
316 bias in canopy height in the discrete return ALS data reported in our study is most likely  
317 caused by the signal processing algorithms used to generate the discrete return products  
318 and has also previously been reported also by Gaveau and Hill (2003). This is a different,  
319 and additional effect to that described by Zimble et al. (2003). Such biases in discrete return  
320 ALS data could be addressed on a site-by-site basis using an empirical calibration against  
321 ground data, although using the waveform allows this bias to be removed in a more  
322 consistent way (Hancock et al., 2011).

323 By adopting a waveform ALS approach, there are benefits and costs for the ecologist. The  
324 major benefits are a more complete three dimensional description of the vegetation canopy.  
325 With waveform data, we show how ecologists can obtain improved canopy height models,  
326 which are critical for improving understanding of spatial carbon assessment and biomass, for  
327 example (Lefsky et al., 2005, Hilker et al., 2010). We also show the potential of the  
328 waveform approach for improved detection and description of understorey characteristics  
329 which are important if spatial models of biodiversity, resource availability (Decocq et al.,  
330 2004), and variables such as propagule abundance and connectivity (Jules and Shahani,  
331 2003) are to be determined. To date, there have only been a limited number of studies that  
332 have investigated canopy understorey characteristics with LiDAR systems, and none  
333 currently exist which use waveform ALS for this purpose. For example, Hill and Broughton  
334 (2009) used leaf-off and leaf-on discrete return ALS data to map the spatial characteristics of  
335 suppressed trees and shrubs growing beneath an overstorey canopy, and Ashcroft et al.  
336 (2014) have demonstrated the capability of TLS to capture three-dimensional vegetation  
337 structure, including understorey. With waveform data we have shown that there exists an  
338 unexplored capability to model canopy understorey in leaf-on stage, over large areal extents:  
339 an exciting scientific opportunity. The costs are a high data storage and processing demand  
340 (see section 3.3) and in this thread there is certainly a great need for more work to improve  
341 and optimize the processing of waveform data to account for multiple scattering effects and  
342 for accounting for the waveform pulse shape. It is also worth noting that currently there are  
343 many LiDAR systems (both ALS and TLS systems) that are waveform-capable but the  
344 waveforms are often discarded during the automated process of generating discrete return  
345 data (e.g. Riegl LMS-Q1560 (Disney et al., 2010)).

346

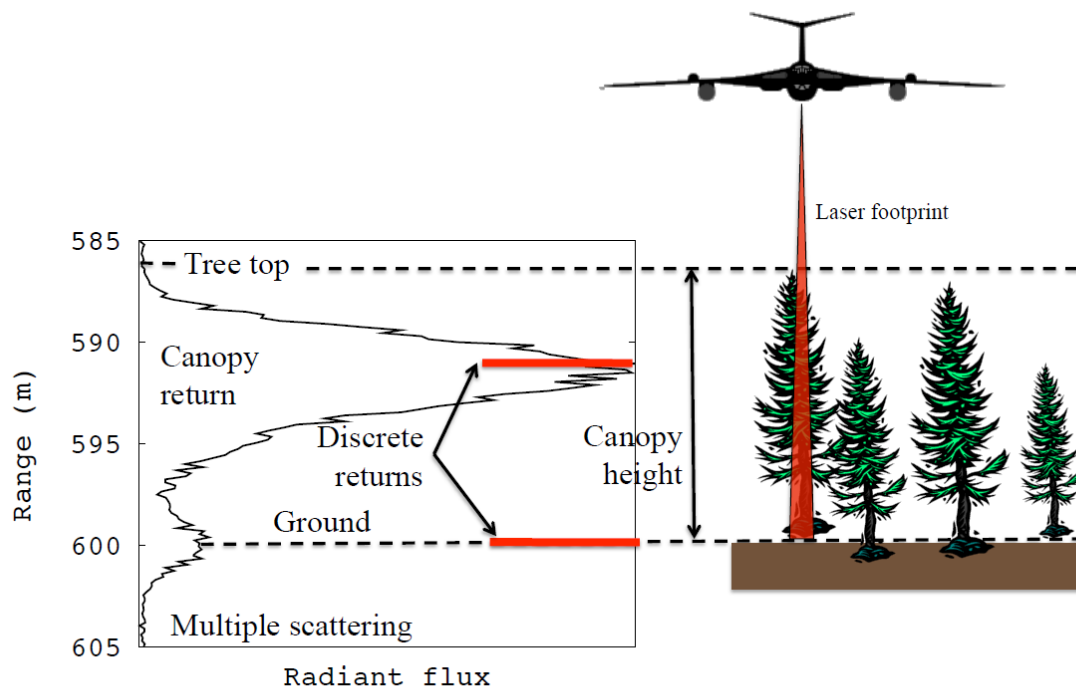
347 In answering the question posed in the title of the paper, we therefore conclude that there is  
348 a hidden and rich resource in data from waveform ALS systems that would provide added  
349 value for spatial ecologists investigating vegetation systems and dynamics across a range of  
350 ecological systems. The 'costs' of processing waveform data should not be overlooked, but a  
351 growing suite of processing tools (table 1) will reduce the processing costs and the technical  
352 requirements for users of waveform data to have signal processing expertise. As waveform  
353 data become more readily available (e.g. through new global missions such as NASA's  
354 GEDI (NASA, 2014, Krainak et al., 2012)) and tools become available to make those data  
355 easier to process, we suggest that these will provide a rich source of accurate, three  
356 dimensional spatial information for describing vegetation canopies. This will improve  
357 scientific understanding of the functional relationships between vegetation structure and  
358 related, important ecological and environmental parameters in a wide range of settings.

359

## 360 **5. Acknowledgements**

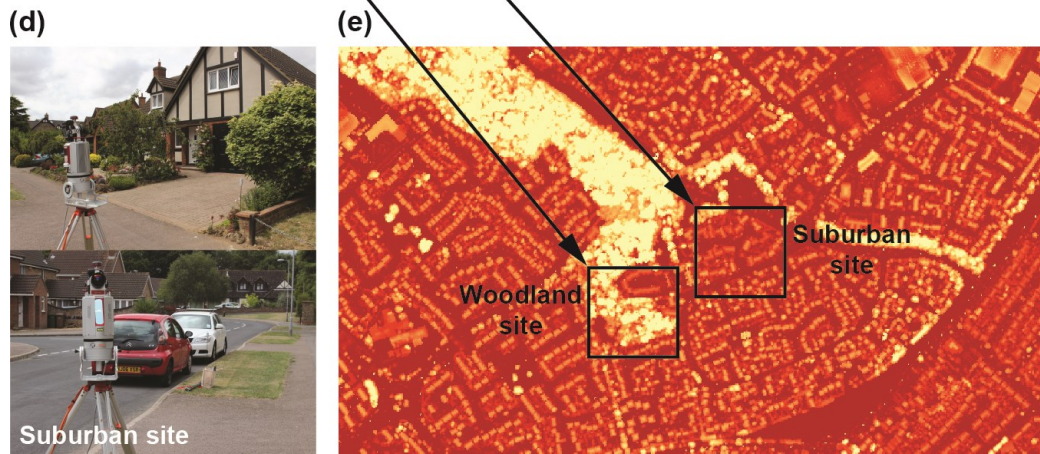
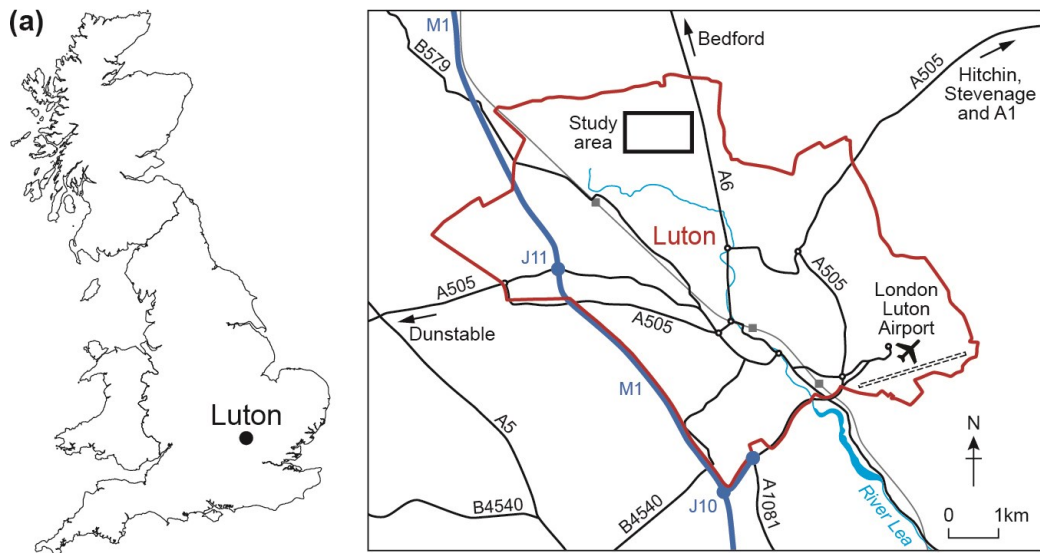
361 This work was funded under the NERC Biodiversity and Ecosystem Services Sustainability  
362 (BESS) thematic programme for the "Fragments Functions and Flows in Urban Ecosystems"  
363 project (Reference: NE/J015237/1; <http://bess-urban.group.shef.ac.uk/>). The waveform ALS  
364 data were acquired by the NERC Airborne Research and Survey Facility (ARSF) and the  
365 team from the ARSF Data Analysis Node at Plymouth Marine Laboratory is acknowledged  
366 for undertaking initial ALS processing. The Riegl VZ-400 TLS used in the validation work is  
367 owned by University College London.

368



369

370 Figure 1: Stylised representation of a waveform ALS system over a tree canopy, showing a  
 371 typical waveform pulse return (left of figure). In contrast, a discrete return system would not  
 372 provide details of the pulse, but would instead report a series of 'hits' from various  
 373 components of the landscape being monitored, typically from near to the top of the tree and  
 374 from somewhere close to the ground surface (sometimes with further returns from points in  
 375 between). Simulated discrete returns are shown on the plot in the left of the figure.



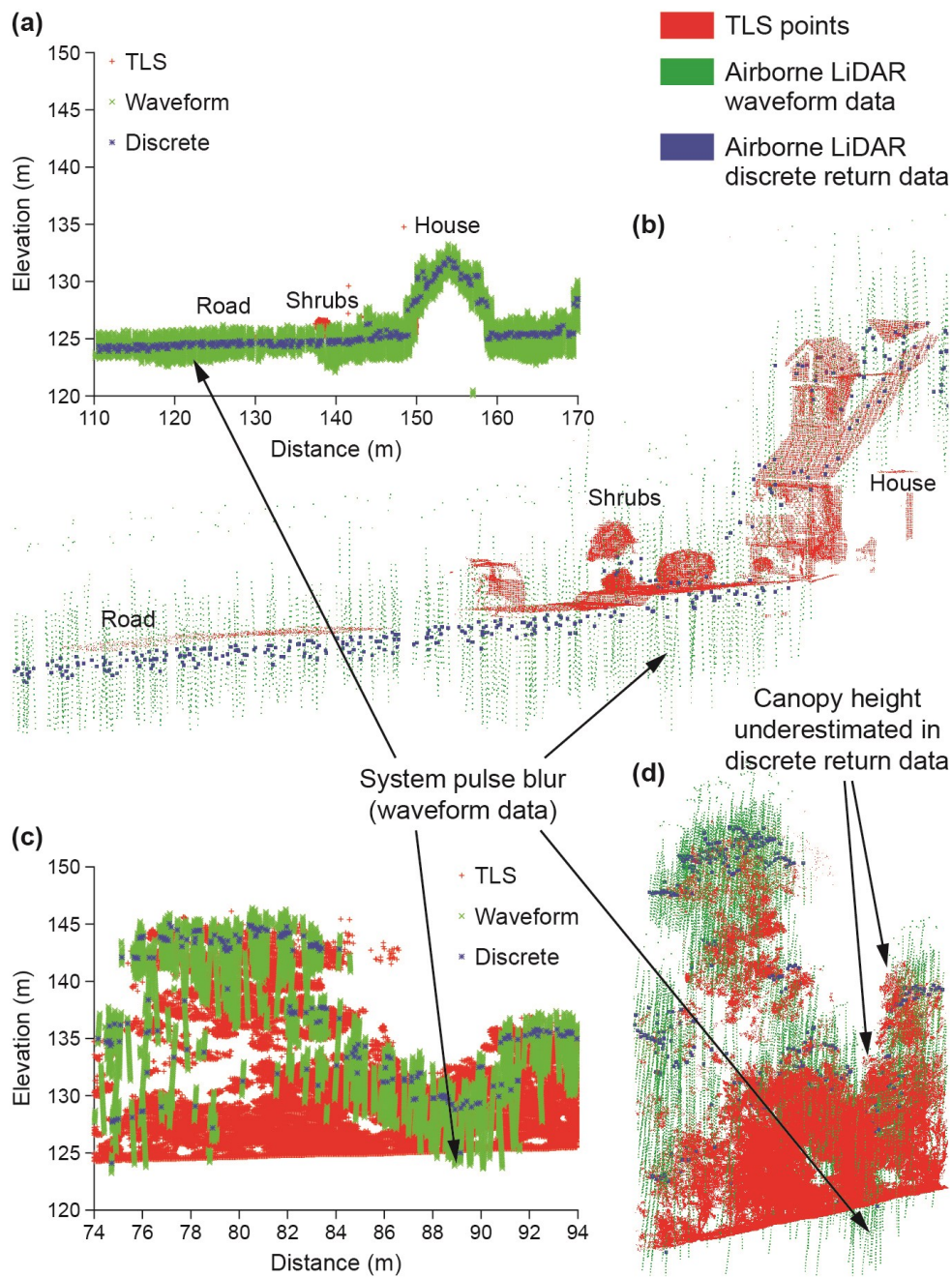
376

377 Figure 2: (a) a map of Luton with position in the UK shown inset, (b) air photo with two urban  
 378 endmember typologies shown, (c) Photographs showing typical vegetation structure at the  
 379 woodland site and (d) at the suburban site, (e) ALS discrete return dataset showing a basic  
 380 vegetation height model of the focus area in Luton, UK.

381

382





383

384 Figure 3: Comparison of TLS, and waveform and discrete return ALS data for two urban  
 385 typologies. (a) and (b) show sections through the 'suburban' scanning site whilst (c) and (d)  
 386 show sections through the 'woodland' scanning site. The simple plots (a) and (c) show a  
 387 cross section through a 2 m deep area, whilst the more complex plots (b) and (d) show a  
 388 cross section through a 20 m deep area to give a broader perspective to the comparison.  
 389 The results highlight where waveform ALS intensity carries information on within-canopy  
 390 structures whilst also demonstrating how discrete return ALS performs best over hard  
 391 surfaces such as roads.

(a) Discrete return ALS intensity



(b) Reflected energy from the waveform ALS data



392

393 Figure 4: The impact of using discrete return intensity vs. waveform ALS in the near infra-red  
394 (1064 nm) is shown for a mixed zone in the focal area of Luton. In (a) the intensity of the  
395 discrete return ALS data are shown, whilst (b) shows the difference when waveform ALS  
396 intensity is used. The major differences in intensity appear in zones with dense vegetation.  
397 These data show that relying on discrete return intensity would lead to bias – the area of  
398 dense trees appear as having low intensity (low reflectance at 1064 nm) when they should  
399 have high reflectance (the two are related). This bias is not present in waveform intensity  
400 which shows both the mown grass and the dense trees as having high intensity which is  
401 correct given the known strong vegetation reflectance response in this region of the  
402 spectrum.

403 Table 1: Summarising free-to-use (FTU) and open-source (O/S) tools for processing and  
 404 visualizing waveform LiDAR data

405

Software	FTU or O/S	Function	Coding expertise required	References
LAStools	FTU	Handling and visualising discrete return LiDAR	Low	<a href="http://www.cs.unc.edu/~isenburg/lastools/">http://www.cs.unc.edu/~isenburg/lastools/</a> (Podobnikar and Vrecko, 2012).
Pulsewaves	FTU	Waveform LiDAR analysis	Low	<a href="http://rapidlasso.com/category/pulsewaves/">http://rapidlasso.com/category/pulsewaves/</a>
SPDLib	O/S	Processing LiDAR data including waveform formats	High, requires C++ coding	<a href="http://www.spdlib.org/doku.php">http://www.spdlib.org/doku.php</a> (Bunting et al., 2013)
PyLAS	O/S	Converts LiDAR formats into GIS layers	Medium, requires Python coding	<a href="https://code.google.com/p/pylas/">https://code.google.com/p/pylas/</a>
LibLAS	O/S	Converts LiDAR formats and links with GDAL functionality	Medium, requires Python coding	<a href="http://www.liblas.org/">http://www.liblas.org/</a>
Cloudcompare	O/S	Visualising 3D LiDAR point clouds	Medium, requires data in specific formats	<a href="http://www.danielgm.net/cc/">http://www.danielgm.net/cc/</a>

406

407

408 **6. References**

409 ALONZO, M., BOOKHAGEN, B. & ROBERTS, D. A. 2014. Urban tree species mapping  
 410 using hyperspectral and lidar data fusion. *Remote Sensing of Environment*, 148, 70-  
 411 83.

412 ANDERSON, J., MARTIN, M. E., SMITH, M. L., DUBAYAH, R. O., HOFTON, M. A., HYDE,  
 413 P., PETERSON, B. E., BLAIR, J. B. & KNOX, R. G. 2006. The use of waveform lidar  
 414 to measure northern temperate mixed conifer and deciduous forest structure in New  
 415 Hampshire. *Remote Sensing of Environment*, 105, 248-261.

416 ANDERSON, K., BENNIE, J. & WETHERELT, A. 2010. Laser scanning of fine scale pattern  
 417 along a hydrological gradient in a peatland ecosystem. *Landscape Ecology*, 25, 477-  
 418 492.

419 ANTONARAKIS, A. S., RICHARDS, K. S. & BRASINGTON, J. 2008. Object-based land  
 420 cover classification using airborne LiDAR. *Remote Sensing of Environment*, 112,  
 421 2988-2998.



422 ARMSTON, J., DISNEY, M., LEWIS, P., SCARTH, P., PHINN, S., LUCAS, R., BUNTING, P.  
423 & GOODWIN, N. 2013. Direct retrieval of canopy gap probability using airborne  
424 waveform lidar. *Remote Sensing of Environment*, 134, 24-38.

425 ASHCROFT, M. B., GOLLAN, J. R. & RAMP, D. 2014. Creating vegetation density profiles  
426 for a diverse range of ecological habitats using terrestrial laser scanning. . *Methods*  
427 *in Ecology and Evolution*, 5.

428 ASNER, G. P., HUGHES, R. F., MASCARO, J., UOWOLO, A. L., KNAPP, D. E.,  
429 JACOBSON, J., KENNEDY-BOWDOIN, T. & CLARK, J. K. 2011. High-resolution  
430 carbon mapping on the million-hectare Island of Hawaii. *Frontiers in Ecology and the*  
431 *Environment*, 9, 434-439.

432 ASPRS. 2015. *LASer (LAS) File Format Exchange Activities - what is the LAS format?*  
433 [[http://www.asprs.org/Committee-General/LASer-LAS-File-Format-Exchange-](http://www.asprs.org/Committee-General/LASer-LAS-File-Format-Exchange-Activities.html)  
434 [Activities.html](http://www.asprs.org/Committee-General/LASer-LAS-File-Format-Exchange-Activities.html)] Date accessed: 3 March 2015 [Online].

435 BOUDREAU, J., NELSON, R. F., MARGOLIS, H. A., BEAUDOIN, A., GUINDON, L. &  
436 KIMES, D. S. 2008. Regional aboveground forest biomass using airborne and  
437 spaceborne LiDAR in Quebec. *Stochastic Environmental Risk Assessment*, 23, 387-  
438 397.

439 BUNTING, P., ARMSTON, J., LUCAS, R. M. & CLEWLEY, D. 2013. Sorted pulse data  
440 (SPD) library. Part I: A generic file format for LiDAR data from pulsed laser systems  
441 in terrestrial environments. *Computers & Geosciences*, 56, 197-206.

442 CALDERS, K., NEWNHAM, G., BURT, A., MURPHY, S., RAUMONEN, P., HEROLD, M.,  
443 CULVENOR, D., AVITABILE, V., DISNEY, M., ARMSTON, J. & KAASALAINEN, M.  
444 2015. Nondestructive estimates of above-ground biomass using terrestrial laser  
445 scanning. *Methods in Ecology and Evolution*, 6, 198-208.

446 CHEN, Z., XU, B. & DEVEREUX, B. 2014. Urban landscape pattern analysis based on 3D  
447 landscape models. *Applied Geography*, 55, 82-91.

448 DANSON, F. M., GAULTON, R., ARMITAGE, R. P., DISNEY, M., GUNAWAN, O., LEWIS,  
449 P., PEARSON, G. & RAMIREZ, A. F. 2014. Developing a dual-wavelength full-  
450 waveform terrestrial laser scanner to characterize forest canopy structure.  
451 *Agricultural and Forest Meteorology*, 198, 7-14.

452 DECOCQ, G., AUBERT, M., DUPONT, F., ALARD, D., SAGUEZ, R., WATTEZ-FRANGER,  
453 A., DE FOUCAULT, B., DELELIS-DUSOLLIER, A. & BARDAT, J. 2004. Plant  
454 diversity in a managed temperate deciduous forest: understorey response to two  
455 silvicultural systems. *Journal of Applied Ecology*, 41, 1065-1079.

456 DISNEY, M., KALOGIROU, V., LEWIS, P., PRIETO-BLANCO, A., HANCOCK, S. &  
457 PFEIFER, M. 2010. Simulating the impact of discrete-return lidar system and survey  
458 characteristics over young conifer and broadleaf forests. *Remote Sensing of*  
459 *Environment*, 114, 1546-1560.

460 DONOGHUE, D. N. M., WATT, P. J., COX, N. J. & WILSON, J. 2007. Remote sensing of  
461 species mixtures in conifer plantations using LiDAR height and intensity data.  
462 *Remote Sensing of Environment*, 110, 509-522.

463 DRAKE, J. B., DUBAYAH, R. O., CLARK, D. B., KNOX, R. G., BLAIR, J. B., HOFTON, M.  
464 A., CHAZDON, R. L., WEISHAMPEL, J. F. & PRINCE, S. D. 2002. Estimation of  
465 tropical forest structural characteristics using large-footprint lidar. *Remote Sensing of*  
466 *Environment*, 79, 305-319.

467 GASTON, K. J., ÁVILA-JIMÉNEZ, M. L. & EDMONDSON, J. L. 2013. REVIEW: Managing  
468 urban ecosystems for goods and services. *Journal of Applied Ecology*, 50, 830-840.

469 GAVEAU, D. L. A. & HILL, R. A. 2003. Quantifying canopy height underestimation by laser  
470 pulse penetration in small-footprint airborne laser scanning data. *Canadian Journal of*  
471 *Remote Sensing*, 29, 650-657.

472 HANCOCK, S., ARMSTON, J., LI, Z., GAULTON, R., LEWIS, P., DISNEY, M., MARK  
473 DANSON, F., STRAHLER, A., SCHAAF, C., ANDERSON, K. & GASTON, K. J.  
474 2015. Waveform lidar over vegetation: An evaluation of inversion methods for  
475 estimating return energy. *Remote Sensing of Environment*, 164, 208-224.

- 476 HANCOCK, S., DISNEY, M., MULLER, J.-P., LEWIS, P. & FOSTER, M. 2011. A threshold  
477 insensitive method for locating the forest canopy top with waveform lidar. *Remote*  
478 *Sensing of Environment*, 115, 3286-3297.
- 479 HANCOCK, S., LEWIS, P., DISNEY, M., FOSTER, M. & MUELLER, J. P. 2008. Assessing  
480 the accuracy of forest height estimation with long pulse waveform lidar through  
481 Monte-Carlo ray tracing. *Proc. SilviLaser 2008, Sept. 17–19, Edinburgh, UK (2008):*  
482 199-206., [available online:  
483 [http://geography.swan.ac.uk/silvilaser/papers/oral\\_papers/Waveform%20LiDAR/Han-](http://geography.swan.ac.uk/silvilaser/papers/oral_papers/Waveform%20LiDAR/Hancock.pdf)  
484 [cock.pdf](http://geography.swan.ac.uk/silvilaser/papers/oral_papers/Waveform%20LiDAR/Hancock.pdf)].
- 485 HARDING, D. J. & CARABAJAL, C. C. 2005. ICESat waveform measurements of within-  
486 footprint topographic relief and vegetation vertical structure. *Geophysical research*  
487 *letters*, 32.
- 488 HILKER, T., VAN LEEUWEN, M., COOPS, N. C., WULDER, M. A., NEWNHAM, G. J.,  
489 JUPP, D. L. B. & CULVENOR, D. S. 2010. Comparing canopy metrics derived from  
490 terrestrial and airborne laser scanning in a Douglas-fir dominated forest stand. *Trees-*  
491 *Structure and Function*, 24, 819-832.
- 492 HILL, R. & BROUGHTON, R. K. 2009. Mapping the understorey of deciduous woodland  
493 from leaf-on and leaf-off airborne LiDAR data: A case study in lowland Britain. *ISPRS*  
494 *Journal of Photogrammetry and Remote Sensing*, 64.
- 495 HOFTON, M. A., MINSTER, J. B. & BLAIR, J. B. 2000. Decomposition of laser altimeter  
496 waveforms. *Ieee Transactions on Geoscience and Remote Sensing*, 38, 1989-1996.
- 497 HOSOI, F., NAKAI, Y. & OMASA, K. 2013. 3-D voxel-based solid modeling of a broad-  
498 leaved tree for accurate volume estimation using portable scanning lidar. *Isprs*  
499 *Journal of Photogrammetry and Remote Sensing*, 82, 41-48.
- 500 HYDE, P., DUBAYAH, R., PETERSON, B., BLAIR, J. B., HOFTON, M., HUNSAKER, C.,  
501 KNOX, R. & WALKER, W. 2005. Mapping forest structure for wildlife habitat analysis  
502 using waveform lidar: Validation of montane ecosystems. *Remote Sensing of*  
503 *Environment*, 96, 427-437.
- 504 HYDE, P., DUBAYAH, R., WALKER, W., BLAIR, J. B., HOFTON, M. & HUNSAKER, C.  
505 2006. Mapping forest structure for wildlife habitat analysis using multi-sensor (LiDAR,  
506 SAR/InSAR, ETM plus , Quickbird) synergy. *Remote Sensing of Environment*, 102,  
507 63-73.
- 508 JIAYING, W., VAN AARDT, J. A. N. & ASNER, G. P. 2011. A Comparison of Signal  
509 Deconvolution Algorithms Based on Small-Footprint LiDAR Waveform Simulation.  
510 *Geoscience and Remote Sensing, IEEE Transactions on*, 49, 2402-2414.
- 511 JONES, D. K., BAKER, M. E., MILLER, A. J., JARNAGIN, S. T. & HOGAN, D. M. 2014.  
512 Tracking geomorphic signatures of watershed suburbanization with multitemporal  
513 LiDAR. *Geomorphology*, 219, 42-52.
- 514 JULES, E. S. & SHAHANI, P. 2003. A broader ecological context to habitat fragmentation:  
515 Why matrix habitat is more important than we thought. *Journal of Vegetation*  
516 *Science*, 14, 459-464.
- 517 KRAINAK, M. A., ABSHIRE, J. B., CAMP, J., CHEN, J. R., COYLE, B., LI, S. X., NUMATA,  
518 K., RIRIS, H., STEPHEN, M. A. & STYSLEY, P. 2012. Laser transceivers for future  
519 NASA missions. *SPIE Defense, Security, and Sensing*, 83810Y-83810Y-11.
- 520 LEFSKY, M. A., COHEN, W. B., PARKER, G. G. & HARDING, D. J. 2002. Lidar remote  
521 sensing for ecosystem studies. *Bioscience*, 52, 19-30.
- 522 LEFSKY, M. A., HARDING, D. J., KELLER, M., COHEN, W. B., CARABAJAL, C. C.,  
523 ESPIRITO-SANTO, F. D., HUNTER, M. O. & DE OLIVEIRA, R. 2005. Estimates of  
524 forest canopy height and aboveground biomass using ICESat. *Geophysical*  
525 *Research Letters*, 32.
- 526 LINDBERG, E., OLOFSSON, K., HOLMGREN, J. & H., O. 2012. Estimation of 3D vegetation  
527 structure from waveform and discrete return airborne laser scanning data. *Remote*  
528 *Sensing of Environment*, 118, 151-161.

- 529 LUSCOMBE, D. J., ANDERSON, K., GATIS, N., WETHERELT, A., GRAND-CLEMENT, E. &  
530 BRAZIER, R. E. 2014. What does airborne LiDAR really measure in upland  
531 ecosystems? *Ecohydrology*.
- 532 MALLET, C. & BRETAR, F. 2009. Full-waveform topographic lidar: State-of-the-art. *ISPRS*  
533 *Journal of Photogrammetry and Remote Sensing*, 64, 1-16.
- 534 NASA. 2014. "New NASA Probe Will Study Earth's Forests in 3-D" (September 8 2014)  
535 [[http://www.nasa.gov/content/goddard/new-nasa-probe-will-study-earth-s-forests-in-](http://www.nasa.gov/content/goddard/new-nasa-probe-will-study-earth-s-forests-in-3-d/)  
536 [3-d/](http://www.nasa.gov/content/goddard/new-nasa-probe-will-study-earth-s-forests-in-3-d/)] Date accessed: 7 April 2015 [Online].
- 537 NERC ARSF. 2014a. Processing report: RG12/10, flight day 249/2012, Luton [[http://arsf-](http://arsf-dan.nerc.ac.uk/trac/ticket/463)  
538 [dan.nerc.ac.uk/trac/ticket/463](http://arsf-dan.nerc.ac.uk/trac/ticket/463)] Date accessed: 7 April 2015 [Online].
- 539 NERC ARSF. 2014b. Processing report: RG12/10, flight day 250/2012, Luton Bedford  
540 [<https://arsf-dan.nerc.ac.uk/trac/ticket/457>] Date accessed: 7 April 2015 [Online].
- 541 PODOBNIKAR, T. & VRECKO, A. 2012. Digital Elevation Model from the Best Results of  
542 Different Filtering of a LiDAR Point Cloud. *Transactions in Gis*, 16, 603-617.
- 543 RONCAT, A., BERGAUER, G. & PFEIFER, N. 2011. B-spline deconvolution for differential  
544 target cross-section determination in full-waveform laser scanning data. *ISPRS*  
545 *Journal of Photogrammetry and Remote Sensing*, 66, 418-428.
- 546 SHUGART, H. H., SAATCHI, S. & HALL, F. G. 2010. Importance of structure and its  
547 measurement in quantifying function of forest ecosystems. *Journal of Geophysical*  
548 *Research-Biogeosciences*, 115.
- 549 VIERLING, K. T., VIERLING, L. A., GOULD, W. A., MARTINUZZI, S. & CLAWGES, R. M.  
550 2008. Lidar: shedding new light on habitat characterization and modeling. *Frontiers in*  
551 *Ecology and the Environment*, 6, 90-98.
- 552 WAGNER, W., HOLLAUS, M., BRIESE, C. & DUCIC, V. 2008. 3D vegetation mapping using  
553 small-footprint full-waveform airborne laser scanners. *International Journal of Remote*  
554 *Sensing*, 29, 1433-1452.
- 555 YAN, W. Y., SHAKER, A. & EL-ASHMAWY, N. 2015. Urban land cover classification using  
556 airborne LiDAR data: A review. *Remote Sensing of Environment*, 158, 295-310.
- 557 ZIMBLE, D. A., EVANS, D. L., CARLSON, G. C., PARKER, R. C., GRADO, S. C. &  
558 GERARD, P. D. 2003. Characterizing vertical forest structure using small-footprint  
559 airborne LiDAR. *Remote Sensing of Environment*, 87, 171-182.

560

561